

1 **Identification of key aroma compounds and core functional microorganisms associated**
2 **with aroma formation for *Monascus*-fermented cheese**

3

4 Yadong Wang^a, Hong Zeng^a, Sizhe Qiu^b, Haoying Han^a, Bei Wang^{a,*}

5^a School of Food and Health, Beijing Technology and Business University, Beijing 100048, China

6^b Department of Engineering Science, University of Oxford, OX1 3PJ, United Kingdom

7*Corresponding author (Bei Wang)

8E-mail: wangbei@th.btbu.edu.cn

9Address: No.11, Fucheng Road, Beijing 100048, China

10Abstract

11This study aimed to analyze the key aroma compounds and core functional microorganisms of
12*Monascus*-fermented cheese (MC). 36 key aroma compounds were identified according to gas
13chromatograph-mass spectrometer (GC-MS), aroma extract dilution analysis (AEDA), and odor
14activity values (OAV) analysis. And internal standard curves were used to clarify the changes in
15their concentration of them during cheese ripening. Furthermore, High-throughput sequencing was
16used to investigate the composition and dynamic changes of bacteria and fungi in MC,
17respectively. *Lactococcus lactis* was found to be the dominant bacterium while *Monascus* was
18confirmed to be the dominant fungus. In addition, Pearson correlation analysis showed that
19*Lactococcus lactis*, *Staphylococcus*, *Trichococcus*, and *Monascus* were strongly associated with
20the 36 key aroma compounds ($r>0.80$, $p<0.05$). Finally, a metabolic network containing
21biosynthetic pathways of the key aroma compounds was constructed. This study provides deeper
22insights into the unique aroma of MC and the contribution of cheese microbiota.

23**Keywords:** *Monascus*-fermented cheese; Gas chromatograph-mass spectrometer (GC-MS); Aroma
24extraction dilution analysis (AEDA); Key aroma compounds; Core functional microorganism;
25Biosynthetic pathways

261. Introduction

27 The *Monascus*-fermented cheese (MC) is a new fermented dairy product that emerged in
282019 (Wu, et al., 2019). The introduction of molds during the cheese ripening stage, e.g.
29*Penicillium roqueforti* in Blue cheeses and *Pen. camemberti* (mainly) in Camembert cheeses, can
30bring stronger proteolytic and lipolytic activities that increase the contents of fatty acids, esters,
31aldehydes, and ketones, which makes cheeses richer in flavor (Kosikowski, 1988). So far, two
32main methods have been reported to make *Monascus*-fermented cheese (Xia, et al., 2020; S.
33Zhang, et al., 2022). One is to imitate the production process of Blue cheese, which makes MC
34with internal mold. The type of MC with internal mold requires a long ripening time to allow
35mold to grow throughout the channels of the cheese, which means that the proteolysis, lipolysis,
36and microbial growth more thoroughly, results in a strong and stimulating odor. The other is to
37simulate the preparation of Camembert cheese which makes MC with surface mold. It has a
38shorter ripening period, with soft sensory qualities such as fruity and milk aroma (S. Zhang, et al.,
392022). Due to the mild flavor and short ripening period, we chose to make a surface-mold ripened
40MC.

41 The variety and contents of flavor compounds are important indicators of cheese quality and
42also key factors that affect consumer preference and consumption choices (Kilcawley, 2017). Due
43to the unique aroma of MC and the potential market value, several works have been conducted to
44investigate the aroma profile and sensory attribute of MC recently (Xia, et al., 2020; S. Zhang, et
45al., 2022). In their work, the content of methyl ketones, esters, and alcohols was high. In addition,
46sensory attribute analysis indicated that the aroma and sensory quality of MC were higher than
47those of commercial blue cheese. Despite previous efforts, there is currently only a preliminary

48understanding of the flavor quality of MC, and there is a lack of research on the key
49(characteristic) aroma compounds of MC. Besides, the specific metabolic pathways that are
50responsible for the formation of those key aroma compounds are still not clear.

51 Cheese is a fermented dairy product, containing different microbial communities, which
52change with time and according to the type of cheese and their respective starter and adjunct
53cultures. These microorganisms are important factors that determine the flavor, quality, and safety
54of cheese products (Santiago-Lopez, et al., 2018; Suzuki-Iwashima, et al., 2020). To make clear
55the relationship between the formation of flavor compounds and microbial communities, previous
56studies have used gas chromatography-mass spectrometry (GC-MS) to resolve the volatile flavor
57compounds (Shi, et al., 2021; Wang, et al., 2021), and then used high-throughput sequencing to
58study microbial communities diversity of fermented foods (Z. Liu, et al., 2020). By analyzing the
59change in aroma compounds and microbial community structure, the function of the microbial
60community over the cheese maturation process and the formation mechanism of aroma
61compounds can be unveiled, which would help improve cheese quality, and lay the foundation for
62cheese standardization. However, the composition of microorganisms and the role of
63microorganisms in the formation of flavor compounds, and the shaping of the overall flavor
64profile of MC have not been reported.

65 In this study, GC-MS, aroma extract dilution analysis (AEDA), odor activity values (OAV)
66analysis, microbial correlation, and metabolic pathway analysis were conducted to obtain a
67quantitative and dynamic understanding of the key aroma compounds and associated functional
68core microbes for MC across a 90-day ripening period. The volatile compounds by GC-MS, the
69qualitative analysis of key aroma compounds by AEDA, and the quantitative determination of key

70aroma compounds by OAV. The time-dependent changes in the composition and abundances of
71bacteria and fungi of MC were identified by 16S rDNA and ITS, respectively. The potential
72correlations between key aroma compounds and microorganisms were uncovered through Pearson
73coefficients, and the core functional microorganisms (i.e. microorganisms strongly associated
74with aroma formation) were determined. Finally, a metabolic network containing the biosynthetic
75pathways of key aroma compounds was assembled referring to the genome-scale metabolic
76networks of *Saccharomyces cerevisiae*, *Lactococcus lactis subsp. cremoris* and *Staphylococcus*
77*aureus subsp. Aureus* and metabolic databases like BiGG and MetaCyc. Overall, this work aims to
78boost the breadth and depth of the current knowledge base of *Monascus*-fermented cheese, which
79would contribute to the development of high-flavor-quality cheeses in the dairy industry.

802. Materials and methods

812.1 Cheese preparation

82 The bovine milk was collected from a local dairy farm. The preparation of MC was
83consistent with our previously published research (Zeng, et al., 2022). The modification was that
84the ripening time of MC was extended. Specifically, the milk was pasteurized at 65°C for 30 min.
85Before renneting, the milk was inoculated with a commercial freeze-dried starter culture (CHR R-
86704, CHR Hansen, Hoersholm, Denmark) and *Monascus purpureus* M1 spore liquid (5.0×10^7
87spores per milliliter) at 31°C and acidified for 60 min. Then, commercial rennet (CHR Hansen,
88Hoersholm, Denmark) was added (0.2 g/L milk) at 31°C for 45 min. The curd was cut into
89approximately 3×3×3 cm cubes. After draining off the whey, NaCl (2.00 g/100 g curd) was added
90to the curd. Then, the curd was placed into square molds and transferred to the incubator (KB450,
91Binder, Tuttlingen, Germany) at 26°C and 70% relative humidity for 5 days, and then at 8°C for

9290 days. Samples were collected at seven different ripening stages (0, 5, 10, 25, 40, 60, and 90
93days) for further analysis. The selection of sampling time was based on the rapid growth of
94microorganisms in the early stage and the significant changes in the cheese, therefore the sampling
95was relatively dense. In the later stage, cheese was in the condition of low-temperature maturation,
96and microbial growth was in a relatively stable stage, so the sampling interval was extended.

972.2 Gas chromatography-mass spectrometry (GC–MS) analysis of volatile compounds

98 The volatile extract of cheese is extracted in two methods, including solvent-assisted flavor
99evaporation (SAFE) and solid-phase microextraction (SPME) -Arrow. For SAFE, the isolation of
100volatiles was according to the previous literature studies with a little modification (Whetstine, et
101al., 2005). Volatile compounds from MC solvent extract with 10 μ L internal standard solution
102containing 2-methyl-pentanoic acid (1266.8 μ g/mL) and 2-methyl-3-heptanone (154.3 μ g/mL)
103dissolved in dichloromethane were distilled. Connected the receiver tube and waste tube to the
104SAFE apparatus. The glassware was then connected to an Edwards nxds6i rotary vane pump as
105the vacuum source. Used a circulating water bath to keep the SAFE apparatus at a constant
106temperature of 40°C. A liquid nitrogen was poured into the cooling trap and the receiver flasks.
107Distillation was carried out for 2 h under vacuum ($\sim 10^{-4}$ Pa). After distillation, the distillate was
108dried over anhydrous sodium sulfate overnight and then concentrated to 1 mL under a gentle
109stream of high-purity nitrogen. The concentrated distillate was washed three times with 1 mL 0.5
110M sodium bicarbonate and mixed thoroughly. After each washing, remove the bottom layer,
111namely the water phase of the distillate, and collect it into a separate test tube. For SPME-Arrow,
112the equilibrium and extraction conditions are as described above (Wang, et al., 2021; Zeng, et al.,
1132022).

114 The GC-MS (Agilent 7890B GC with Agilent 5977A Mass Selector Detector, Agilent
115 Technologies, Santa Clara, California America) analyses parameters were consistent with previous
116 studies (Zeng, et al., 2022). For SAFE, injected the liquid directly into the injection port. For
117 SPME-Arrow, inserted the extracted fiber into the injector port and used the splitless mode.
118 Samples were analyzed on both a DB-Wax column (60 m × 0.25 mm i.d. × 0.25 μm film, Agilent
119 Technologies, Santa Clara, California America), and the injector port was held at 230°C. The
120 column carrier gas was helium at a constant flow rate of 1.2 mL/min. The oven temperature was
121 held at 40°C for 5 min, increased to 230°C at a rate of 3°C/min. The mass spectrometer was
122 operated in the electron impact mode with 70 eV ionization energy, and the source temperature
123 was set at 230°C. Full-scan acquisition was used in the 30 to 350 m/z range. High-purity helium
124 (99.99%) was applied as the carrier gas for GC-MS analysis. Each analysis was performed in
125 triplicate.

126 2.3 Aroma extraction dilution analysis (AEDA)

127 For SAFE, the volatile extracts of MC were diluted stepwise with dichloromethane in serial
128 dilutions of 1:3¹, 1:3², 1:3³, and so forth. For SPME-Arrow, Dilution analysis was performed by
129 changing the GC inlet split ratio, which was set to 1:3¹, 1:3², 1:3³, and so forth. Three experienced
130 panelists (two females and one male) used chromatography–olfactometry (GC–O), an Agilent
131 7890B series GC coupled with a sniffing system (ODP 3 Gerstel, Mülheim, North Rhine-
132 Westphalia, Germany), for sensory evaluation of each dilution until no aroma was perceived, with
133 corresponding dilution factors (FD) of 3, 9, 27, ..., and 3ⁿ, respectively (H. Zhang, et al., 2022).

134 2.4 Quantitative analyses of key aroma compounds

135 Internal standard curves were constructed using GC-MS for the quantitative analysis of the
136 key aroma compounds. Selective ion monitoring MS was adopted. To get more accurate

quantitative results, a matrix to simulate MC was prepared with milk protein concentrate powder, water, and sunflower oil and used for matrix-matched recovery during analytical quantification (Wang, et al., 2021). The MPC/water/oil simulant matrix was prepared as follows: first, the milk protein concentrate powder (MPC 70, Saishang Dairy Company, Ningxia, China) and ultrapure water were mixed and pasteurized as the substrate. Then the substrate was incubated with rennet (CHY-MAX Powder Extra, Hensel, Germany) at 31°C until it coagulated. The fresh curd was prepared by the whey draining process, then freeze-dried and crushed in a grinder for later use. The crushed curd (protein phase), deodorized sunflower oil (fat phase), and ultrapure water (water phase) were mixed in the same proportion as in MC. 2-methyl-pentanoic acid (0.923 µg/µL in n-hexane for quantitation of carboxylic acids) and 2-methyl-3-heptanone (0.816 µg/µL in n-hexane for quantitation of other compounds) were added into the *Monascus*-fermented cheese matrix as the internal standards. The specific amount of addition to the internal standard depends on the type of compound to be quantified. To homogenize the internal standard in the sample, the MPC/water/oil simulant matrix was ground twice in a stirrer for 30 seconds each time. Then, according to the semiquantitative results of MC samples in the pre-experiment, the concentration gradient of each compound was set and added successively, and the standard curve of no less than 5 points was established. All standard curves were constructed by plotting the ratio of the peak area of the reference compound to the peak area of the internal standard against its concentration (Zhang, et al., 2018).

The calculation formula for the concentration of volatile compounds is

$$f = \frac{A_s/m_s}{A_r/m_r},$$

158 where A_s is the peak area of the internal standard compound, A_r is the peak area of the
159 compound under test, m_s is the mass of the internal standard compound, m_r is the mass of the
160 compound under test, and f is the average value of the calibration factor calculated for each
161 concentration of the standard.

162 2.5 Odor activity values (OAV)

163 The olfactory intensity of each compound in the sample is highly correlated with its
164 concentration and odor threshold. In this study, the odor activity values (OAV) were used to
165 describe the intensity of odor compounds in the sample. The OAV is the ratio of the concentration
166 of a single compound to the odor threshold of that compound. (Trabue, et al., 2006). When a
167 compound has $OAV > 1$, it is considered to contribute to the overall aroma of the sample. The
168 compound threshold used in this study is from references. (Gemert, 2013; Wang, et al., 2021)

169 2.6 Microbial analysis

170 Before extracting, 1 g of the sample was ground in a sterile quartz mortar for 2 min and
171 homogenized with 9 mL of sterile NaCl solution (0.85%, wt/vol) for 10 min. To separate fat and
172 coarse particles, the suspension was centrifuged at $5,000 \times g$ for 10 min at 4°C, and 1 g of the
173 upper sediment was collected into a sterile microcentrifuge tube using a sterile spoon. Total
174 genomic DNA was extracted using the Qiagen DNA Mini kit (Qiagen, Dusseldorf, North Rhine-
175 Westphalia, Germany) according to the manufacturer's protocol. The concentration and purity of
176 the extracted DNA were determined using a Nanodrop ND 1000 spectrophotometer (Thermo
177 Fisher Scientific, Wilmington, America) and 1.0% agarose gel electrophoresis, respectively.
178 Samples were stored at -20°C.

179 For bacteria (Zhong, et al., 2018), the V3–V4 domains of 16S rDNA were amplified by PCR
180 using primer pairs 515F (5'-GTGYCAGCMGCCGCGGTAA-3') and 806R (5'-

181GGACTACHVGGGTWTCTAAT-3') with specific barcode. For fungi (Zhong, et al., 2018), the
182ITS1 rDNA regions were amplified by PCR (95°C for 2 min, followed by 30 cycles at 95°C for 30
183s, 61°C for 30 s, and 72°C for 45 s with a final extension at 72°C for 10 min) with the primers
184ITS5F (5'-GGAAGTAAAAGTCGTAACAAGG-3') and ITS2R (5'-
185GCTGCGTTCTTCATCGATGC-3') with specific barcode. Further paired-end sequencing was
186performed using an Illumina MiSeq instrument (Illumina Inc., San Diego, California, America).

1872.7 Determination of free fatty acids (FFAs)

188 The fatty acids (FFAs) extraction and methylation were performed according to Balthazar
189(Balthazar, et al., 2016). Collect the derived fatty acid (FAME) in hexane in dichloromethane and
190pass a 0.45 injection-µm Filter before injection for GC-MS analysis. The initial temperature was
19150°C and held for 3 minutes, then ramped up to 160°C at 6°C/min and then to 250°C at 2°C/min
192for 1 minute. Helium was used as the carrier gas at a flow rate of 1.0 mL/min. The temperature of
193the ion source was 200°C. The mass scan range was 30-500 m/z and the electron energy was 70
194eV. The content of FFA is obtained from the peak area of the total ionic current.

1952.8 Determination of organic acids

196 The extraction method of organic acids in MC refers to Bouzas with slightly modified
197(Bouzas, et al., 1993). 5 g of MC was weighed into 25 ml of 0.009N H₂SO₄ and stirred for 1 hour.
198Then centrifuge (5000 × g, 10 min) and filter the supernatant through a 0.2 mm membrane filter
199(Gelman). The sample volume of 10 µL. The mobile phases were 0.1% phosphoric acid and
200acetonitrile (8:2). The absorbance was 210 nm, the column temperature was 35°C, the flow rate
201was 1 mL/min, and the elution is 40 min. 14 organic acids (formic acid, oxalic acid, tartaric acid,
202malic acid, lactic acid, acetic acid, citric acid, succinic acid, maleic acid, fumaric acid, and pyruvic
203acid) were used as external standards.

2042.9 Determination of free amino acids (FAAs)

205 30 mg samples of cheese freeze-dried powder in different ripening periods were taken, and
206 analyzed the content of free amino acids was by HPLC. Chromatographic analysis conditions:
207 Zorbax Eclipse-AAA chromatographic column (4.6 mm × 150 mm, 5 μm); Mobile phase: A: 40
208 mmol/L NaH₂PO₄ (pH=7.8), B: Acetonitrile: methanol: water (45:45:10, V: V: V); Injection
209 volume: 10 μL; Column temperature: 40°C. Detection wavelength: 338 nm. Qualitative and
210 quantitative analysis with the mixed free amino acid standard.

2112.10 Data analysis

212 All statistical analyses were performed with three biological replicates. One-way ANOVA
213 followed by Duncan's multiple tests was used to verify significant differences in key aroma
214 compounds at a level of $p < 0.05$ (the Statistical Program for the Social Sciences 23.0; SPSS Inc.,
215 Chicago, IL, America). Additionally, the microbial abundance, microbial diversity, and Pearson
216 correlation analysis were performed using the OriginPro 2021 64-bit (OriginPro Lab Corp.,
217 Northampton, America). Linear discriminant analysis Effect Size (LEfSe) using Galaxy for
218 analysis (<http://huttenhower.sph.harvard.edu/galaxy/>). The correlation network of microorganisms
219 and environmental compounds was visualized using Gephi 0.9.

2203. Results and discussion

2213.1 Aroma profiles of *Monascus*-fermented cheese

2223.1.1 Characterization of volatile aroma compounds

223 To obtain an overview of the evolution of the aroma profile of *Monascus*-fermented cheese
224 (MC) across the 90-day ripening period, the volatile aroma compounds of MC ripened for 0 days,
225 5 days, 10 days, 25 days, 40 days, 60 days, and 90 days were analyzed by SPME-Arrow-GC-MS.
226 Clustering analysis showed that the complete 90-day ripening period can be divided into four

227stages: 0 days (unripened/fresh cheese), 5-10 days, 25-60 days, and 90 days (Fig.1).
228Correspondingly, MC ripened for 0, 10, 40 and 90 days were selected as representations of each
229stage for further analysis (see below).

230 To obtain more comprehensive information on the volatile aroma compounds, two different
231extraction methods were used, i.e. solid-phase microextraction (SPME) -Arrow and solvent-
232assisted flavor evaporation (SAFE). SPME-Arrow has higher stability, longer service life, 6 times
233the adsorption area, and 10 times the sensitivity (Kremser, et al., 2016), which is suitable for
234extracting low boiling point compounds. SAFE is suitable for extracting high boiling point
235compounds. Combining the results of SPME-Arrow and SAFE, a total of 85 volatile aroma
236compounds were detected in MC across the 90-day ripening period (Fig.1), including 20 acid
237compounds, 27 ester compounds, 13 ketone compounds, and 42 other compounds.

2383.1.2 Determination of flavor dilution (FD) factors of key aroma compounds

239 Gas chromatography-olfactometry can be conducted to evaluate the relative contribution of
240odorants by AEDA, being based on threshold concentrations in air (Gemert, 2013; Wang, et al.,
2412021). The results of AEDA in MC with different ripening stages were shown in Table S1.

242 During the ripening process, a total of 36 volatile aroma compounds had FD factor ≥ 81 (the
243FD of the compound in one or more stages is greater than or equal to 81), which were identified as
244the key aroma compounds of MC. Specifically, 12 aroma compounds with FD factor ≥ 81 were
245found in unripened MC (day 0). Among them, butanoic acid (pungent, FD = 243) and decanoic
246acid (rancid, FD = 243) had the highest FD factors, indicating their key role in the overall aroma
247at this stage. In addition, pentanoic acid (sour, FD = 81), hexanoic acid (sour and cheesy, FD =
24881), octanoic acid (rancid, FD = 81), benzoic acid (sour, sulfur, and musty, FD = 81) mainly
249contributed to the sour and cheesy flavors while 2-Heptanone (fruity and creamy, FD = 81) and 2-

250tridecanone (fruity, creamy, FD = 81) contributed to the fruity and creamy flavors in unripened
251MC. δ -Decanolactone (fruit and wine aroma, FD = 81), limonene (lemon, FD = 81), and benzene
252ethanol (fruity, alcohol, FD = 81) contributed to the fruity, alcoholic flavors in unripened MC
253(Wang, et al., 2021).

254 Moving on to the second stage of the whole ripening period (represented by MC sampled on
255day 10), 26 aroma compounds with FD factor ≥ 81 were detected. Among them, butanoic acid
256(pungent, FD = 729), octanoic acid (rancid, FD = 279), decanoic acid (rancid, FD = 729), and
257dodecanoic acid (lemon and sour, FD = 729) had the highest FD factors, which showed that acid
258compounds are still the most important aroma compounds of MC at the initial stage of the
259ripening process. Following, acetic acid (sour and vinegar, FD = 243), 3-methyl-butanoic acid
260(sour, FD = 243), heptanoic acid (sour and cheesy, FD = 243), nonanoic acid (sour and cheesy, FD
261= 243) contributed to the sour and cheesy flavors. Decanoic acid ethyl ester (wine and apple, FD =
262243), 2-tridecanone (fruity, creamy, FD = 243), 2-pentanone (fruit, creamy, FD = 81), 2-heptanone
263(fruit and wine aroma, FD = 81), 2-decanone (fruit and wine aroma, FD = 81), and hexanoic acid
264hexyl ester (fresh vegetable, FD = 81) contributed to fruity and creamy flavors in MC. δ -
265Decanolactone (fruit and wine aroma, FD = 243), δ -dodecalactone (fruit and wine aroma, FD =
266243), octanoic acid ethyl ester (fruit and wine aroma, FD = 81), contributed to fruity and wine
267flavors. Limonene (lemon, FD = 81) contributed to lemon flavors. 2,3-butanediol (fruity, buttery,
268FD = 243), and benzene ethanol (fruity, alcohol, FD = 243) contributed to the fruity, alcoholic
269flavors.

270 For the third stage of ripening (represented by MC sampled on day 40)), there were 29 aroma
271compounds with FD factor ≥ 81 found in MC. Among them, decanoic acid (rancid, FD = 729),

272butanoic acid (pungent, FD = 729), octanoic acid (rancid, FD = 729), decanoic acid, ethyl ester
273(wine and apple, FD = 729), 2-tridecanone (fruity, creamy, FD = 729) and δ -decanolactone (fruit
274and wine aroma, FD = 729) had the highest FD factor. During this stage, esters and ketones have
275become important aroma compounds of MC. The FD factor of acid compounds in MC decreased
276slightly, while the FD factor of ester compounds and ketone compounds increased. The decrease
277in acid may be due to the activation of the esterification reaction, which converts the accumulated
278short-chain fatty acids into esters (Xu, et al., 2020). As for the ketones, recalling the biochemical
279reactions that occurred in Blue cheese, acid compounds can undergo β -oxidation and be converted
280to methyl ketone by lipoxygenase (Kranz, et al., 1992). Correspondingly, in this work, we saw that
281the FD factors of ketone compounds in MC increased as the FD factors of acids decreased.

282 Finally, for the last stage of ripening (represented by MC sampled on day 90), there were 25
283aroma compounds with FD factor ≥ 81 in MC. Among them, butanoic acid (pungent, FD = 729),
2842-tridecanone (fruity, creamy, FD = 729), and 3-hydroxy-2-butanone (fruity, creamy, FD = 729)
285had the highest FD factors. During this stage, the FD factor of most acid compounds in MC
286continued to decrease. Ketones were still the important aroma compounds in MC.

2873.1.3 Quantification of key aroma compounds and their OAV

288 To better assess the contribution of key aroma compounds, further calculations of odor
289activity values (OAV) were carried out for 36 key aroma compounds with FD ≥ 81 . OAV is an
290important indicator for the quantitative evaluation of the contribution of volatile compounds to
291food aroma.

292 The results of the OAVs of 36 key aroma compounds in MC were listed in Table 1, which
293showed a similar trend to the AEDA results. 14 compounds were found with OAV ≥ 1 for
294unripened MC (sampled on day 0), including hexanoic acid, octanoic acid, decanoic acid, 2-

295heptanone, 2-nonanone, 2-undecanone, 3-hydroxy-2-butanone, δ -decanolactone, δ -dodecalactone,
296limonene, benzaldehyde, benzene ethanol, and 1-dodecanol. Notably, no ester compounds were
297presented at the beginning of the ripening process. As ripening proceeded, more and more ester
298compounds developed, such as hexanoic acid ethyl ester, hexanoic acid butyl ester, and octanoic
299acid ethyl ester.

300 The number of aroma compounds with $OAV \geq 1$ increases to 33, 36, and 33 for MC ripened
301for 10 days, 40 days, and 90 days, respectively. Most of them are acids, esters, and methyl
302ketones. Among these compounds, hexanoic acid ethyl ester has the highest OAV (4843.76) on
303day 40, followed by butanoic acid ($OAV = 1112.93$, day 40) and 2-heptanone ($OAV = 1094.68$,
304day 10). It has been reported that these compounds are important flavor contributors of other
305mold-ripened cheese, such as Blue cheese, Brie cheese, and Camembert cheese (Suzuki-Iwashima,
306et al., 2020). But the difference is that the content of these compounds in MC is about multiple
307higher than that of corresponding compounds in Blue cheese, Brie cheese, and Camembert cheese
308(Karahadian, et al., 1985; S. Zhang, et al., 2022). For example, the content of the ester compounds
309in MC is about 4 times as much as that in Blue cheese(Lawlor, et al., 2003; S. Zhang, et al., 2022).
310Therefore, esters, acids, and methyl ketones are the key aroma compounds in MC, which have
311important contributions to cheese senses. The implication is that the aroma quality of MC may be
312richer and softer compared to cheeses, such as Blue cheese and aged Cheddar cheese, dominated
313by acid compounds.

314 Considering the AEDA and OAV analysis in combination, except for unripened MC, the key
315aroma compounds of MC with different ripening stages were similar, including acids compounds
316(acetic acid, butanoic acid, pentanoic acid, hexanoic acid, heptanoic acid, octanoic acid, nonanoic

317acid, decanoic acid, undecanoic acid, benzoic acid, and dodecanoic acid), ester compounds (318hexanoic acid ethyl ester, hexanoic acid butyl ester, octanoic acid ethyl ester, nonanoic acid ethyl 319ester, hexanoic acid hexyl ester, decanoic acid ethyl ester, and dodecanoic acid ethyl ester), ketone 320compounds (2-pentanone, 2-heptanone, 2-octanone, 2-decanone, 2-undecanone, 2-tridecanone, 321and 3-hydroxy-2-butanone), other compounds (γ -octalactone, δ -decanolactone, δ -dodecalactone, 322limonene, styrene, 2,3-butanediol, benzaldehyde, benzene ethanol, and 1-dodecanol). However, 323the amount of these compounds continuously changed with the MC ripening process. Specifically, 324acid compounds, such as hexanoic acid, octanoic acid, and decanoic acid, contribute more to the 325volatile flavor of cheese on 0 and 10 days of ripening. As ripening proceeded, more and more 326ester compounds and ketone compounds developed, such as hexanoic acid ethyl ester, hexanoic 327acid butyl ester, 2-pentanone, and 2-octanone.

3283.2 Microbiological analysis of *Monascus*-fermented cheese

329 Microorganisms play an important role in the formation of cheese aroma. This study 330characterized the composition and dynamic changes of microbial abundances and investigated the 331different stages of ripening (0 days, 10 days, 40 days, 90 days) of MC.

3323.2.1 Analysis of bacterial diversity during the ripening process

333 63 genera were detected at the level of bacterial community genera in MC. As shown in 334Fig.2A, the top 10 species in the genus level were *Lactococcus*, *Staphylococcus*, *Lactobacillus*, 335*Streptococcus*, *Bifidobacterium*, *Alloprevotella*, *Bacteroides*, *GpI*, and *Barnesiella*. Among them, 336*Lactococcus* and *Staphylococcus* were the main dominant species during ripening. *Lactococcus* 337was the dominant group with the largest proportion. Its relative abundance ranged from 90.33% to 33898.50%. The relative abundance of *Lactococcus* first decreased, then increased, and reached the 339highest on day 90. *Staphylococcus* was the second dominant bacteria in MC, but its relative

340abundance was far from that of *Lactococcus*. It only accounted for 0.090% on day 0 and reached
341the maximum value of 6.60% on day 10. Then, gradually decreased, accounting for 2.96% and
3420.21% on day 40 and day 90, respectively. The changing trend of the relative abundance of
343*Staphylococcus* was opposite to that of *Lactococcus*.

344 Analysis of the microbiota α -diversity (indicated by Shannon index) indices suggests that the
345microbial diversity of MC sampled on day 10 was significantly higher than that at other periods
346($p < 0.05$) (Fig.2B). After day 10, it was observed that the Shannon index decreased significantly,
347and the species diversity was the lowest on day 90, which may be resulted from the high relative
348abundance of *Lactococcus* at that time. In addition, based on the weighted uniFrac distance metric,
349 β -diversity analysis showed a significant difference between the 10-day group and other groups
350($p < 0.05$) (Fig.2C).

351 LEfSe could analyze the differences between groups of bacteria and find out the types of
352microorganisms with differences between groups (Fig.2D) (Zhao, et al., 2022). 20 biomarkers
353with LDA scores > 2 were obtained after LEfSe analysis of MC ripened for 0, 10, 40, and 90 days.
354*Lactococcus*, *Streptococcaceae*, and *Lactobacillales* were identified as biomarkers at the genus
355level in the 90-day group (LDA scores greater than 4). Finally, the cluster thermogram analysis
356was carried out to show the differences in the species composition of MC at different ripening
357periods. As shown in Fig.2E, 0-day and 10-day groups can be clustered together, while the rest
358two can be grouped into one, indicating that the bacterial species and content in MC changed
359significantly within cluster 1 (0-10 day) to cluster 2 (40-90 day).

3603.2.2 Analysis of fungi diversity during the ripening process

361 A total of 103 genera were detected at the level of the fungi community genera in MC across
362the 90-day ripening period. As shown in Fig.3A, the top 10 species in the genus level were

363 *Monascus*, *Meyerozyma*, *Fusarium*, *Mortierella*, *Funneliformis*, *Aspergillus*, *Gibellulopsis*,
 364 *Cladosporium* and *Plectosphaerella*. *Monascus* and *Meyerozyma* are the main dominant fungi,
 365 accounting for more than 99% of the overall abundance. The relative abundance of *Monascus* first
 366 increased and then decreased from day 0 to day 90, being 46.54%, 81.41%, 53.42%, and 54.47%
 367 respectively. On the other hand, the relative abundance of *Meyerozyma* was 52.70% on day 0,
 368 decreased to 18.16% on day 10, and increased significantly and became stable on day 40 and day
 369 90, with the proportion of 46.21% and 45.19%, respectively.

370 The analysis of the fungi α -diversity index of MC at different ripening periods showed that
 371 the Shannon index on day 10 was significantly lower than that on day 0, day 40, and day 90 ($p <$
 372 0.05), indicating that the fungi diversity at this time points decreased (Fig.3B). This may be due to
 373 the high proportion of *Monascus* and *Meyerozyma* at this time. The β -diversity analysis based on
 374 the weighted uniFrac distance metric showed that the β -diversity of the 90-day group was
 375 significantly higher than that of the others ($p < 0.05$) (Fig.3C). Fig.3D showed that 0-day, 10-day,
 376 and 40-day were clustered into one group, and the 90-day was significantly different from other
 377 groups in species composition. The LEfSe analysis results of fungi were not shown as the LDA
 378 scores of fungi were less than 2.

379 3.3 Metabolomics analysis of *Monascus*-fermented cheese

380 Free fatty acids (FFAs) were a major group of metabolites that related to flavor formation
 381 during cheese ripening. Long-chain unsaturated fatty acids can be further oxidized and
 382 decomposed to produce aromatic compounds such as aldehydes, alcohols, and ketones, which lead
 383 to flavors in fermented products. Apart from FFAs, organic acids are another major group of
 384 compounds that are closely related to flavor formation in cheeses. The organic acids themselves

385have a fruit acid aroma at low concentrations and pungent sour at high concentrations. In addition,
386the organic acids produced during cheese ripening can be esterified with alcohols to form esters,
387which not only provide an enhanced aroma but also reduces the irritating taste of organic acids
388(Li, et al., 2020). In addition, free amino acids (FAAs) were metabolic precursors of volatile sulfur
389compounds, aldehydes, ketones, and fatty acids, which also play an important role in the
390formation of cheese aroma (Izco, et al., 2000).

391 In this work, the dynamic changes in the concentrations of FFAs in MC were determined via
392GC-MS, and the dynamic changes in the concentrations of organic acids and FAAs in MC were
393determined via high-performance liquid chromatography (HPLC). The production and
394accumulation of high concentrations of FFAs and organic acids were observed in MC across the
39590-day ripening period. 23 kinds of FFAs were identified (Table S2), among which oleic acid
396(C18:1) was the most abundant one. It has been suggested that oleic acid can undergo autoxidation
397and convert into nonanal, octanal, and other aldehydes (Zhao, et al., 2022). In addition, high levels
398of linoleic acid (C18:2), myristic acid (C14:0), palmitic acid (C16:0), and stearic acid (C18:0)
399were also found. As for organic acids, lactic acid, pyruvic acid, citric acid, oxalic acid, maleic
400acid, and tartaric acid were detected (Table S2). The content of lactic acid is 30121.84 mg/kg on
401day 40, which is mainly produced by glycolysis of halophilic microorganisms, such as
402*Staphylococcus* (S. Liu, et al., 2019). In addition, the content of tartaric acid in MC was also found
403to be at a high level (6152.24 mg/kg) on day 40. As shown in Table S3, During the ripening of
404MC, a total of 15 FAAs was detected, and the total content increased first, then on day 40
405decreased. Among them, glutamic acid (Glu), phenylalanine (Phe), and leucine (Leu) were higher,
406accounting for 45.99% of the total FAAs in MC. Glutamic acid is a common flavor enhancer in

407foods, which can cooperate with GMP and IMP to enhance the umami taste characteristics of
408cheese (Phat, et al., 2016). Phenylalanine and leucine are bitter amino acids that may bring
409bitterness to the cheese. But as important precursors of related aroma compounds, they also have a
410positive effect on cheese flavor development.

4113.4 The correlation between flavor metabolites and microorganisms

412 During the fermentation process of MC, the flavor metabolites and microorganisms changed
413dynamically with the ripening process. Pairwise correlation analysis was performed for flavor
414metabolites and microorganisms to analyze the potential interaction (Qian, et al., 2023). Pearson
415correlation coefficients revealed that the populations of several microorganisms were significantly
416correlated with the abundance of flavor metabolites ($|r| > 0.60$, $p < 0.05$) (Fig.4A). *Lactococcus*,
417*Staphylococcus*, *Trichococcus*, *Monascus* showed significant correlations with δ -dodecalactone,
418pentanoic acid (C5:0), hexanoic acid (C6:0), tridecanoic acid (C13:0), pentadecanoic acid (C15:0),
419hexadecanoic acid (C16:0), nonadecanoic acid (C19:0), heneicosanoic acid (C21:0), 10-methyl
420nonadecanoic acid (C19:1), maleic acid, citric acid, tartaric acid, lactic acid, and leucine (Leu). In
421addition, *Muribaculaceae*, *Lactobacillus*, *Bacteroides*, *Alistipes*, *Limnohabitans*, *Enterococcus*,
422*Faecalibacterium*, *Meyerozyma*, *Candida*, *Aspergillus*, *Russula*, *Fusarium*, *Mycoclamys*,
423*Mortierella*, *Chaetomium*, and *Preussia* showed significant negative correlations with oxalic acid,
424lactic acid, hexanoic acid butyl ester (Butyl ester- C6:0), 2-tridecanone, eicosanoic acid (C20:0),
425valine (Val), proline (Pro), asparagine (Asp), phenylalanine (Phe), leucine (Leu), and arginine
426(Arg). Among these paired connections, *Lactococcus*, *Staphylococcus*, *Trichococcus*, and
427*Monascus* had strong significant positive correlations with flavor metabolites ($r > 0.80$, $p < 0.05$),
428which may be used as the core functional microorganism in MC.

429 Detailed visualization of significant correlations was presented as an undirected network
430graph (Fig.4B). In bacteria, *Lactococcus*, the dominant genus, had significant positive correlations
431with δ -dodecalactone and C6:0. Previous works have also indicated that *Lactococcus* is an
432important source of δ -lactones in fermentation (Zia, et al., 2022). *Staphylococcus* had significant
433positive correlations with several fatty acids, such as maleic acid and citric acid. Research on
434mixed culture in fermented meat indicated that *Staphylococcus* has high lipase activity to generate
435free fatty acids, which contributes to flavor formation (Lawlor, et al., 2003). In addition,
436*Trichococcus* positively correlated with tartaric acid, C5:0, and Leu. The high positive correlation
437between *Trichococcus* and tartaric acid was also observed in other correlation studies for flavor
438metabolites and microbial communities (Sacks, et al., 2018). The positive correlations between
439*Trichococcus* and C5:0 and Leu were not reported by previous studies as found. There were fewer
440significant positive correlations between fungi and metabolites: only *Monascus* was positively
441correlated with lactic acid and C5:0. Though lactic acid bacteria usually would be major lactic
442acid-producing organisms in fermented food, *Monascus* could also act as a "cell factory for lactic
443acid production" (Santiago-Lopez, et al., 2018).

444 Concerning significant negative correlations, oxalic acid negatively correlated with most
445bacteria and fungi, C20:0 negatively correlated with almost all bacteria except *Lactococcus*,
446*Staphylococcus*, and *Trichococcus*, and proline showed significant negative correlation with all
447fungi except *Monascus* and bacteria including *Enterococcus*, *Limnohabitans*, and
448*Faecalibacterium*. In previous research on antimicrobial compounds from fungi extracts, oxalic
449acid was detected to exhibit antibacterial activity against phytopathogenic bacteria, such as
450*Streptococcus faecalis* (minimal inhibitory concentrations = 10 μ g/mL – \geq 128 mg/L) (Alves, et

451al., 2012). C20:0 (30 μ M/10 mL of Nutrient Broth) also showed antimicrobial activity against
452pathogenic infection in existing studies (Bravo-Santano, et al., 2019). In addition, proline-rich
453peptides (2 to 8 mg/L) have been found to have an antibiotic effect against bacteria like
454Enterobacteriaceae in a few previous research works (Luzia, et al., 2018). Therefore, oxalic acid,
455C20:0, and proline-rich peptides might act as anti-microbial agents for unwanted microorganisms
456in cheese. In the future, to accurately evaluate the association between flavor metabolites and
457microorganisms during the ripening of MC, the core functional microbiota responsible for the
458production of volatile aroma should be further explored.

4593.5 Formation of flavor metabolites in *Monascus*-fermented cheese based on microbial metabolic 460network

461 The metabolic network containing biosynthetic pathways of flavor metabolites, including
462short-chain carboxylic acids (lactic acid, citric acid, oxalic acid, maleic acid, and tartaric acid),
463saturated and unsaturated fatty acids, fatty acid derivatives (hexanoic acid butyl ester, 2-
464tridecanone, and δ -dodecalactone) and amino acids (Pro, Phe, Asp, Arg, Leu, and Val), was
465assembled referring to genome-scale metabolic networks of *Saccharomyces cerevisiae*, and gram-
466positive bacteria, such as *Lactococcus lactis subsp. cremoris* and *Staphylococcus aureus subsp.*
467*aureus*, BiGG database, MetaCyc database, and previous works on biosynthesis of flavor
468metabolites.

469 Short-chain carboxylic acids, e.g., lactic acid, mostly derive from intermediates of glycolysis,
470for example, the biosynthesis of oxalic acid starts from phosphoenolpyruvate and D-Erythrose 4-
471phosphate (Fig.5A). Maleic acid and tartaric acid can both be synthesized from fumarate, an
472intermediate of the TCA cycle. Maleate cis-trans isomerase (MALEI) catalyzes the conversion of

473 fumarate to maleic acid. Another biosynthetic pathway of maleic acid presented in the genome-
 474 scale metabolic network of *Staphylococcus aureus subsp. aureus* suggests that maleic acid can be
 475 formed by the oxidation of nicotinate through nicotinic acid 6 hydroxylase (NACHY),
 476 (6HNACMO), 2,5-dihydroxypyridine dioxygenase (PYRDOX), N-Formyl maleate deformylase
 477 (NFMLDF) and pyrazinamidase (PYRZAM) (Becker, et al., 2005). For tartaric acid, the
 478 epoxidation of fumarate (FUMEPO) forms epoxy succinic acid, and then cis-epoxy succinate
 479 hydrolase (CESH) catalyzes the dehydration of epoxy succinic acid (Xuan, et al., 2019).

480 The biosynthesis of fatty acids and their derivatives are all initiated by acetyl-CoA
 481 (coenzyme A), which formed malonyl-ACP with bicarbonate by acetyl-CoA carboxylase
 482 (ACCOA) and malonyl-CoA-ACP trans acylase (MCOATA) (Fig. 5B). Malonyl-ACP is the
 483 building block of both even and odd-numbered fatty acids: the elongation of even-numbered ones
 484 starts from C4:0 (butanoic acid) and malonyl-ACP, and that of odd-numbered ones starts from
 485 C3:0 (propionic acid) and malonyl-ACP. Fatty acid derivatives (i.e., esters and ketones) were
 486 found to correlate significantly with microorganisms in MC were hexanoic acid butyl ester, 2-
 487 tridecanone, and δ -dodecalactone. Hexanoic acid butyl ester derives from C6:0 (hexanoic acid) by
 488 butyl esterification (BTES60), which is common in microorganisms. For 2-tridecanone, the
 489 dehydration of 3-oxotetradecanoyl-CoA by thioester hydrolase (THH) forms its precursor, 3-oxo-
 490 myristate, and then, the decarboxylation catalyzed by 3-monolaurate decarboxylase (OXGDC3,
 491 EC 4.1.1.56) forms 2-tridecanone. Previous studies have indicated that 2-tridecanone was
 492 synthesized by bacteria instead of fungi (Mohan, et al., 2020). No significant positive
 493 correlation of 2-tridecanone or hexanoic acid butyl ester (butyl ester C6:0) was found in section
 494 3.4 to show its possible source. δ -dodecalactone is a δ -lactone formed by the lactonization of 5-

495hydroxy alkanoic acid (5HDCALAC) (Zia, et al., 2022), which is 5-hydroxydodecanoic acid in
496this case.

497 The biosynthesis of amino acids is mainly mediated by aminotransferases, such as aromatic
498amino acid aminotransferase phenylalanine (araphe), transaminase, and ornithine transaminase
499(ORNTA) (Fig. 5C). Proline can be synthesized from L-Glutamate 5-semialdehyde (glu5sa)
500through L-glutamate 5-semialdehyde dehydratase (G5SADs) and pyrroline-5-carboxylate (P5CR),
501and glu5sa can be formed either from glutamate through glutamate 5-kinase (GLU5K) and
502glutamate-5-semialdehyde dehydrogenase (G5SD), or from 2-oxoglutarate and ornithine through
503ornithine transaminase (ORNTA). The removal of an amino group by L-asparaginase (ASNN)
504from asparagine forms aspartate, and then aspartate and citrulline can form argininosuccinate, the
505precursor of arginine, by arginine-succinate synthase (ARGSS). And argininosuccinate lyase
506(ARGSL) will split argininosuccinate to produce arginine. With phenylpyruvate (phpyr), also
507involved in the synthesis of oxalic acid, as the precursor, phenylalanine can be formed by the
508transfer of the amino group from other amino acids such as tyrosine. Similarly, Leu and Val can be
509synthesized from 4-Methyl-2-oxopentanoate and 3-Methyl-2-oxobutanoate respectively. Only the
510significant positive correlation between *Trichococcus* and Leu suggests the potential source of
511Leu, other amino acids' sources cannot be deduced from the correlation analysis in section 3.4.

5124. Conclusion

513 A total of 36 key aroma compounds of *Monascus*-fermented cheese (MC) were identified
514during ripening. Among them, acid compounds, such as hexanoic acid octanoic acid, and decanoic
515acid contribute more to the volatile flavor of cheese on 0 and 10 days of cheese ripening. As
516ripening proceeded, more and more ester compounds and ketone compounds developed, such as

517hexanoic acid ethyl ester, hexanoic acid butyl ester, 2-pentanone, and 2-octanone. In addition,
518*Lactococcus lactis* and *Monascus* were the dominant bacterium and fungus in MC, respectively.
519Furthermore, Pearson correlation analysis suggested that *Lactococcus lactis*, *Monascus*,
520*Staphylococcus*, and *Trichococcus*, were strongly associated with δ -dodecalactone, hexanoic acid,
521and pentanoic acid (members of the 36 key aroma compounds, $r>0.80$, $p<0.05$), and was identified
522as the core functional microorganisms. Finally, a metabolic network containing biosynthetic
523pathways of key aroma compounds concluded that short-chain carboxylic acids mostly derive
524from intermediates of glycolysis, and the biosynthesis of fatty acids and their derivatives (i.e.,
525esters and ketones) are all initiated by acetyl-CoA. The biosynthesis of amino acids is mainly
526mediated by aminotransferase. This study constitutes a more comprehensive atlas of *Monascus*-
527fermented cheeses via quantifying the key aroma compounds, core functional microorganisms,
528and the metabolic pathways towards the formation of key aroma compounds, which can contribute
529to the development of potential strategies to improve the flavor quality of mold-ripened cheeses.

530 Acknowledgements

531 This work was supported by National Natural Science Foundation of China (project No.
532 32072345; Beijing) and the Cultivation Project of Double First-Class Disciplines of Food Science
533 and Engineering, Beijing Technology & Business University (BTBUYXTD202205).

534 Abbreviations:

535 MC, *Monascus*-fermented cheese; GC-MS, Gas chromatograph-mass spectrometer; AEDA,
536 Aroma extract dilution analysis; OAV, Odor activity values; SPME-Arrow, Solid-phase
537 microextraction Arrow; SAFE, Solvent-assisted flavor evaporation.

538 Author contributions

539 Yadong Wang: Formal analysis, Methodology, Writing—original draft and editing. Hong
540 Zeng: Methodology, Writing—review and editing, Supervision. Sizhe Qiu: Writing—original draft
541 and editing. Haoying Han: Writing—original draft and editing. Bei Wang: Supervision, Validation,
542 Methodology, Writing—review and editing, Funding acquisition, Project administration.

543 Conflicts of Interest

544 The authors declared that they have no conflicts of interest to this work.

545 Data Availability

546 The raw data supporting the conclusions included in the article can be obtained from the
547 corresponding author upon reasonable request.

548 Reference

549

550Tables and figures

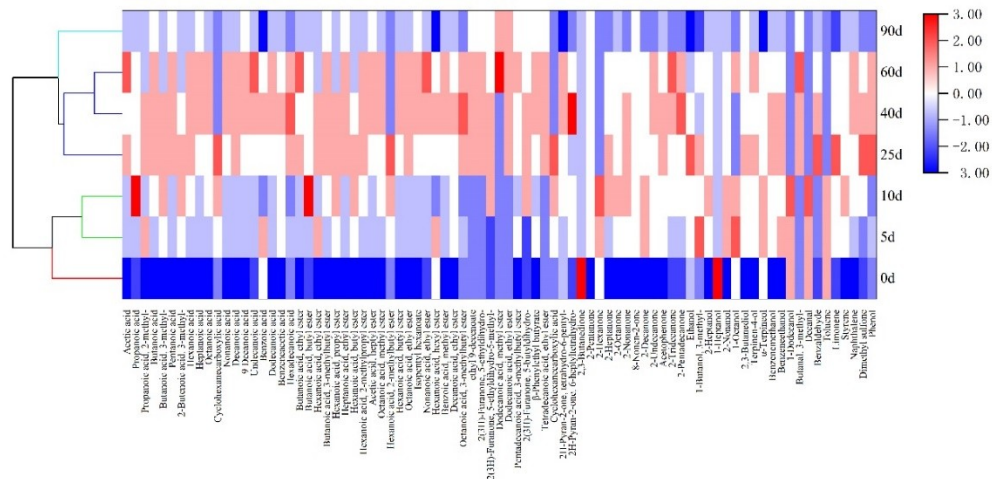
551Table 1 Quantitation and odor activity values (OAV) of key aroma compounds in *Monascus*-
552fermented cheese. Abbreviation: 0d, 10d, 40d, 90d refers to cheese ripened for 0 day, 10 days, 40
553days, and 90 days, respectively.

Compounds	Concentration (±SD) (µg/kg)				Threshold ¹ (µg/kg)	OAV			
	0d	10d	40d	90d		0d	10d	40d	90d
Acids									
Acetic acid	523.87±	4348.1±	3029.76±	2188.79±	700	0.75	6.21	4.33	3.13
	18.63	1207.36	305.97	409.52					
Butanoic acid	-	2513276.38	3338781.1±	1187692.05	3000	23.58	837.76	1112.93	395.9
		±279129.31	191432.83	±235689					
3-Methyl-butanoic acid	-	286114.93±	315179.64±	93072.73±	1000	-	286.11	315.18	93.07
		202689.54	100063.98	28051.73					
Pentanoic acid	-	11955.97±	19311.89±	10320.86±	9000	-	1.33	2.15	1.15
		46282.7	143761.66	278841.12					
Hexanoic acid	11199.08±	626329.85±	688624.63±	155018.19±	4300	2.6	145.66	160.15	36.05
	1481.82	73102.74	46940.46	55584					
Heptanoic acid	254.96±	9152.04±	20097.31±	7136.13±	640	0.4	14.3	31.4	11.15
	30.34	3994.86	3325.32	1725.43					
Octanoic acid	7048.69±	125731.29±	131813.01±	44499.06±	3000	2.35	41.91	43.94	14.83
	792.13	45366.71	33641.82	7237.25					
Nonanoic acid	957.36±	10157.12±	31860.03±	7838.69±	8800	0.11	1.15	3.62	0.89
	222.89	4680.78	7001.97	2275.58					
Decanoic acid	29676±	438920.88±	917612.43±	182675.37±	2300	12.9	190.84	398.96	79.42
	6300.09	183055.72	124206.46	57984.68					
Undecanoic acid	93.4±	494.9±	895.07±	236.94±	100	0.93	4.95	8.95	2.37
	11.22	182.24	102.21	47.82					
Benzoic acid	769.62±	778.1±	7648.22±	239.43±	1000	0.77	0.78	7.65	0.24
	229.68	23.87	3825.43	105.81					
Dodecanoic acid	4011.13±	75144.96±	2459.37±	36659.72±	10000	0.4	7.51	4.21	3.67
	1242.34	8851.45	910.7	8256.78					
Esters									
Hexanoic acid, ethyl ester	-	4998.95±	14531.27±	5798.92±	3	-	1666.	4843.	1932.
		3519.56	3151.7	1607.14					
Hexanoic acid, butyl ester	-	257.66±	598.46±	429.57±	70	-	3.68	8.55	6.14
		446.27	49.26	3.28					
Octanoic acid, ethyl ester	-	2212.39±	13130.27±	5097.73±	960	-	2.3	13.68	5.31
		997.13	1125.17	1007.44					
Nonanoic acid, ethyl ester	-	-	287.36±	283.97±	50	-	5.92	2.59	1.7
			60.21	13.76					
Hexanoic acid, hexyl ester	-	295.89±	129.61±	85.1±	1	-	295.89	129.61	85.1
		36.29	5.55	3.62					

Decanoic acid, ethyl ester	-	242.47± 225.59	4218.54± 869.78	1614.47± 428.51	530	-	0.46	7.96	3.05
Dodecanoic acid, ethyl ester	-	-	652.03± 131.46	358.64± 261.06	2	-	-	326.02	179.32
Ketones									
2-Pentanone	-	13512.56± 256.46	6731.38± 118.45	2905.68± 472.04	1380	-	9.79	4.88	2.11
2-Heptanone	1258.28± 41.76	25177.56± 6984.67	6210.18± 1600.4	1718.47± 162	23	54.71	1094. 68	270.01	74.72
2-Octanone	-	2172.09± 659.31	899.16± 97.73	566.64± 17.67	50	-	43.44	17.98	11.33
2-Nonanone	740.19± 39.86	24159.58± 12521.58	10988.25± 1978.68	2962.06± 337.93	200	3.7	120.8	54.94	14.81
2-Decanone	-	1859.47± 832.32	804.02± 171.93	196.68± 18.72	110	-	16.9	7.31	1.79
2-Undecanone	438.25± 33.56	3491.68± 990.37	1821.6± 243.41	620.63± 32.33	10	43.83	349.17	182.16	62.06
2-Tridecanone	-	189.33± 5.43	157.49± 4.39	102.94± 2.23	1	-	189.33	157.49	102.94
2-Butanone, 3-hydroxy-	1087.13± 340.43	4168.13± 2475.63	2642.49± 473.92	1003.42± 884.98	14	77.65	297.72	188.75	71.67
Others									
γ-Octalactone	-	251.27± 300.49	199.02± 58.93	23.74± 4.15	20	-	12.56	9.95	1.19
δ-Decanolactone	62.61± 55.47	297.4± 28.32	222.68± 90.21	36.68± 3.93	50	1.25	5.95	4.45	0.73
δ-Dodecalactone	4710.42± 1296.31	16908.59± 5045.8	18359.09± 6727.92	5682.26± 1431.58	100	47.1	169.09	183.59	56.82
Limonene	111.54± 96.62	458.09± 96.91	279.48± 35.66	163.84± 2.67	70	1.59	6.54	3.99	2.34
Styrene	-	18604.51± 2377.14	4839.02± 755.08	1023.72± 35.18	70	-	265.78	69.13	14.62
2,3-Butanediol	-	87.68± 151.86	2058.66± 433.62	283.02± 16.47	3	-	29.23	686.22	94.34
Benzaldehyde	489.31± 31.12	2159.59± 314.94	3709.81± 390.72	1151.38± 232	60	8.16	35.99	61.83	19.19
Benzene ethanol	10010.55± 11594.39	629432.06± 284276.66	489171.04± 193940.69	98774.66± 55268.44	390	25.67	1613. 93	1254.28	253.27
1-Dodecanol	270.65± 6.04	316.24± 21.53	3068.17± 58.83	213.35± 184.8	16	16.92	19.76	191.76	13.33

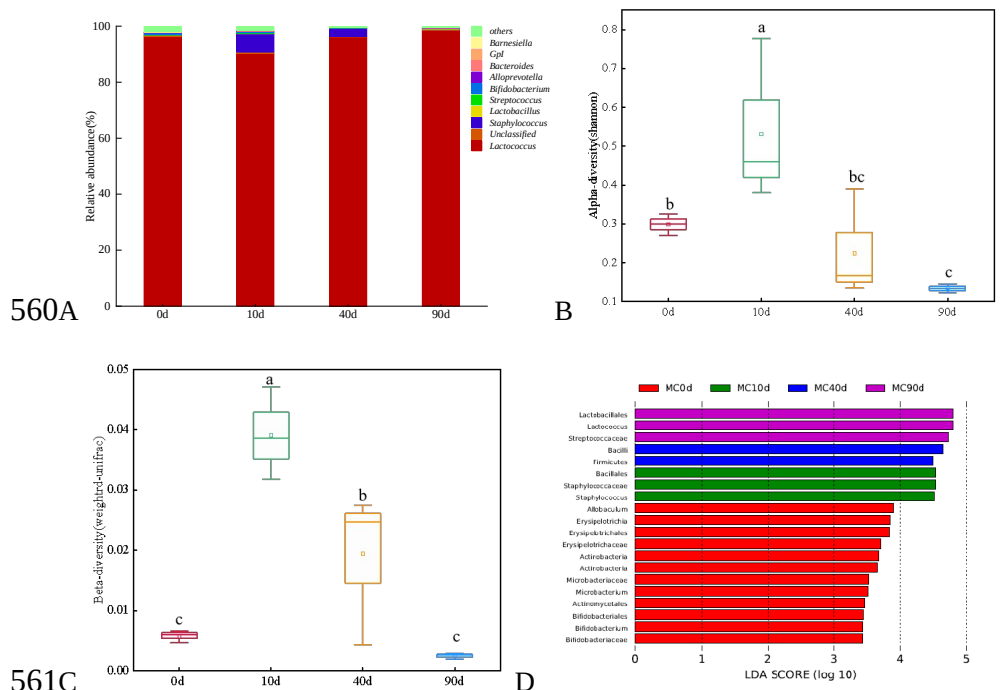
554¹Threshold from the literature (Gemert, 2013; Wang, et al., 2021).

555"- means not detected.



556

557 Fig.1 Heat map of the relative contents of volatile aroma compounds in *Monascus*-fermented
 558 cheese (MC) across the 90-day ripening. Data presented in the heat map are in the log10 scale. 0d:
 559 MC ripened for 0 day.

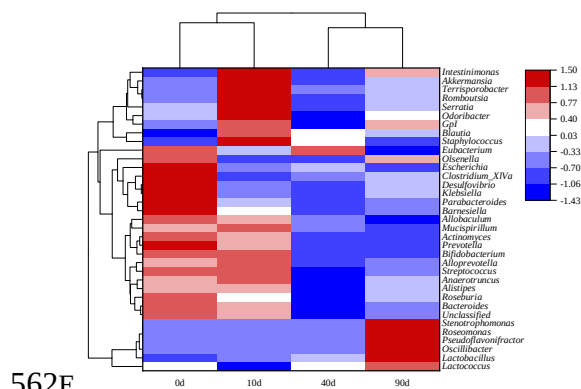


560A

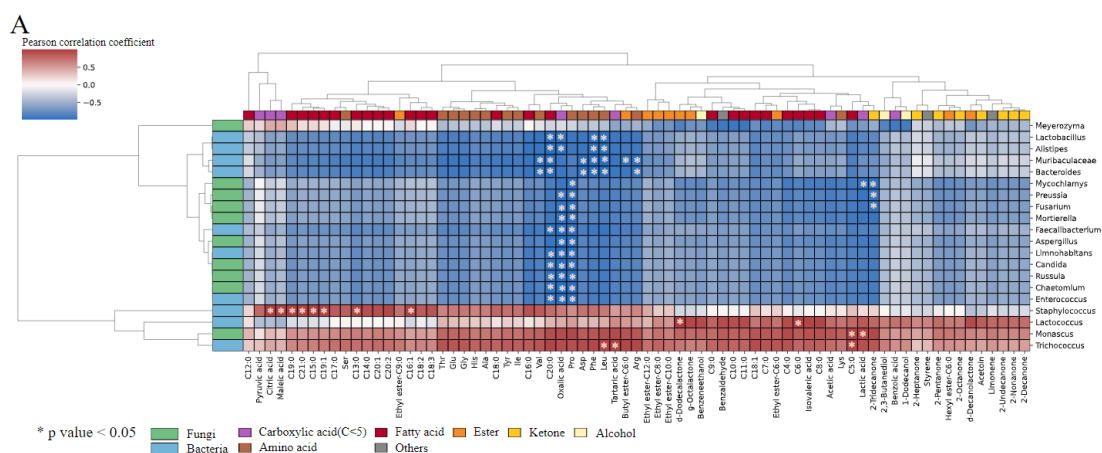
B

561C

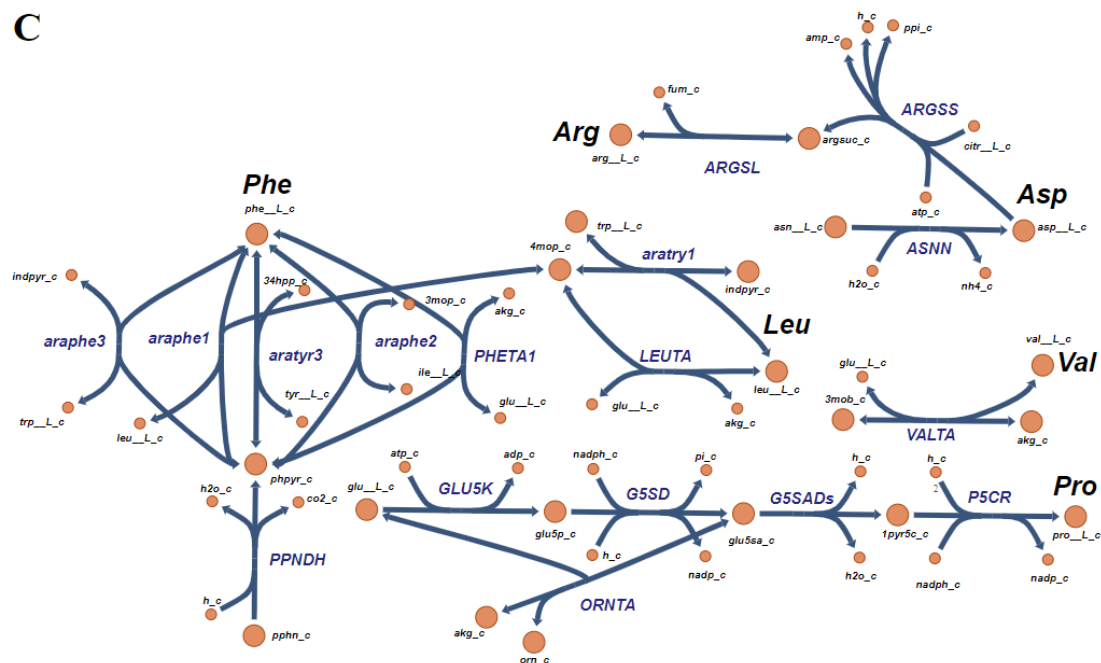
D



562E



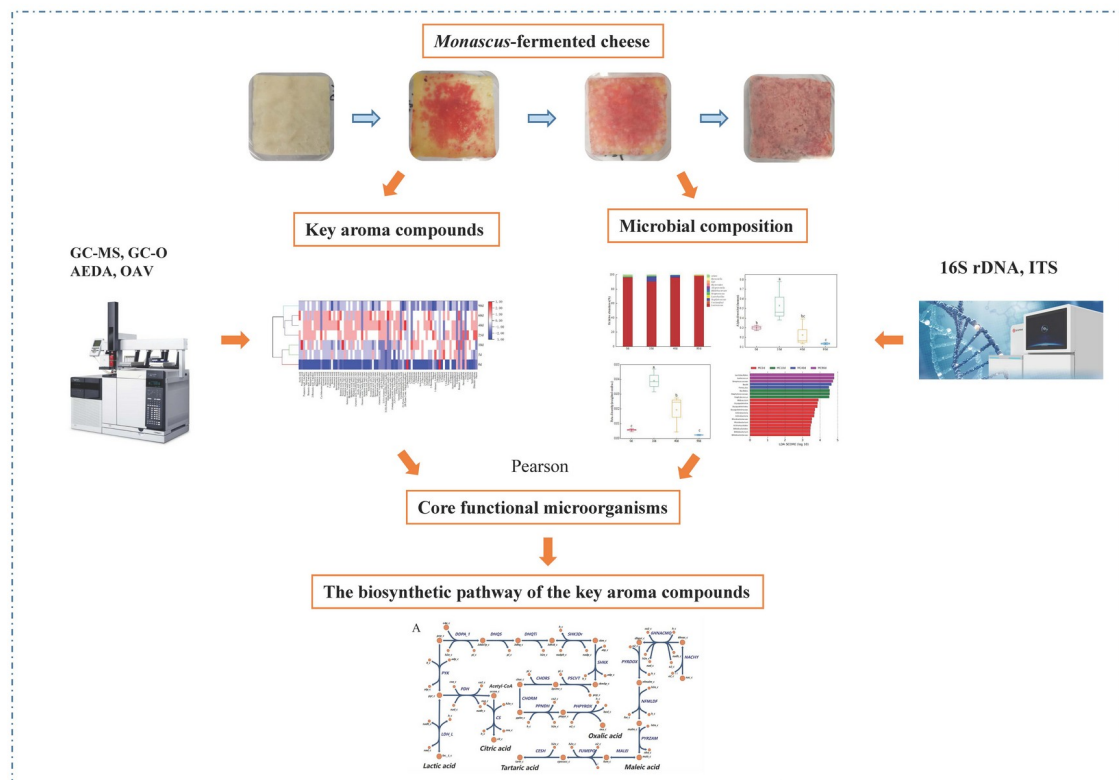
C



590

591 Fig.5. Biosynthetic pathways of short-chain carboxylic acids (A), medium-chain fatty acids,
 592 esters, ketones (B) and amino acids (C) that showed significant correlations with microorganisms
 593 in this study. Corresponding Table S4 for compound abbreviations. The blue letters in the figure
 594 represent enzymes, which were sourced from the BiGG database and MetaCyc database.

595 Graphical abstract



596